



Cite this: *Phys. Chem. Chem. Phys.*, 2015, 17, 18269

Received 23rd May 2015,  
Accepted 22nd June 2015

DOI: 10.1039/c5cp02985f

[www.rsc.org/pccp](http://www.rsc.org/pccp)

**By using solid-state  $^{17}\text{O}$  NMR spectroscopy, we provide the first direct experimental evidence for bonds between Al and non-bridging oxygen (NBO) ions in aluminosilicate glasses based on rare-earth (RE) elements, where RE = {Lu, Sc, Y}. The presence of  $\sim 10\%$  Al–NBO moieties out of all NBO species holds regardless of the precise glass composition, at odds with the conventional structural view that Al–NBO bonds are absent in highly polymerized and Si-rich aluminosilicate glass networks.**

Owing to their importance for both materials and earth sciences, vast efforts have been spent to improve the structural understanding of aluminosilicate (AS) glasses.<sup>1</sup> Ternary  $\text{M}_{(2)}\text{O}-\text{Al}_2\text{O}_3-\text{SiO}_2$  glasses normally involve a monovalent alkali ( $\text{M}^+$ ) or divalent alkaline-earth ( $\text{M}^{2+}$ ) metal cation. The glass networks comprise  $\text{SiO}_4$  and  $\text{AlO}_4$  tetrahedra that are cornershared by bridging oxygen (BO) atoms. The additional negative charge of each  $\text{AlO}_4^-$  moiety (relative to  $\text{SiO}_4$ ) requires nearby cations for attaining local charge-balance, while the remaining  $\text{M}^{2+}$  cations depolymerize the glass network by converting BO ( $\text{O}^{[2]}$ ) atoms into non-bridging oxygen (NBO;  $\text{O}^{[1]}$ ) species.<sup>1</sup> The relative BO/NBO speciations in melts and glasses dictate many properties, such as viscosity, conductivity, and thermal expansion.<sup>1,2</sup>

The following three features of the structural understanding of AS glasses have prevailed for decades, all building around the consequences of the excess negative charge of the  $\text{AlO}_4$  groups:<sup>1,2</sup> (i) Both Si and Al are four-fold coordinated ( $\text{Si}^{[4]}$  and  $\text{Al}^{[4]}$ ) by O, except if the network-modifier content is insufficient for balancing the entire Al speciation as  $\text{Al}^{[4]}$ ; then, higher-coordination  $\text{AlO}_5$  and  $\text{AlO}_6$  polyhedra form whenever  $zn_{\text{M}} < n_{\text{Al}}$  or  $n_{\text{Si}} < n_{\text{Al}}$ ,<sup>1,2</sup> where  $n_{\text{E}}$  denotes the stoichiometric amount of element E in the glass and  $z$  is the charge of  $\text{M}^{2+}$ . (ii) To avoid local negative charge-accumulation in the structure, there is a strong preference for  $\text{Si}^{[4]}-\text{O}-\text{Al}^{[4]}$  linkages, whereas those of  $\text{Al}^{[4]}-\text{O}-\text{Al}^{[4]}$  are absent (the “Loewenstein rule”<sup>3</sup>). (iii) Moreover, there is a dominance of

## Direct $^{17}\text{O}$ NMR experimental evidence for Al–NBO bonds in Si-rich and highly polymerized aluminosilicate glasses<sup>†</sup>

Aleksander Jaworski, Baltzar Stevensson and Mattias Edén\*

Si–NBO contacts relative to Al–NBO, implying that all NBO species are accommodated by  $\text{SiO}_4$  in silica-rich AS glasses.<sup>1,4</sup>

However, over the past decade, violations of properties (i)–(ii) are well documented for AS glasses based on mono/di-valent cations, where several studies reveal minor fractional populations of  $\text{AlO}_5$  groups (a few %) in fully charge-balanced ( $n_{\text{M}} = n_{\text{Al}}/z = n_{\text{Si}}/z$ ) “tectosilicate” AS glasses<sup>4c,5</sup> (notwithstanding that glasses formed at high pressure reveal significant  $\text{AlO}_5/\text{AlO}_6$  populations<sup>6</sup>). Moreover, while Loewenstein’s rule holds strictly for crystalline AS phases featuring  $n_{\text{Al}} \leq n_{\text{Si}}$  (such as zeolites and minerals<sup>1a</sup>), minor deviations thereof are reported for  $\text{M}_{(2)}\text{O}-\text{Al}_2\text{O}_3-\text{SiO}_2$  glasses.<sup>7</sup> Yet, whereas the early literature identified the preference of Si–NBO over Al–NBO associations, the existence of the latter were often deduced from circumstantial evidence.<sup>2</sup> Nevertheless, property (iii) is nowadays assumed to apply universally for any  $\text{SiO}_2$ -dominated  $\text{M}_{(2)}\text{O}-\text{Al}_2\text{O}_3-\text{SiO}_2$  glass. Direct experimental evidence for Al–NBO contacts only exist for amorphous M–Al–O aluminates, or AS glasses that are simultaneously rich in network-modifiers and  $\text{Al}_2\text{O}_3$ , while  $\text{SiO}_2$  is a minor component (<40 mol%).<sup>4</sup>

However, the presence of trivalent rare-earth ( $\text{RE}^{3+}$ ) cations in  $\text{RE}_2\text{O}_3-\text{Al}_2\text{O}_3-\text{SiO}_2$  glasses<sup>8</sup> leads to markedly higher configurational and chemical disorder, as mirrored in the following structural features: (1) significant  $\text{AlO}_5/\text{AlO}_6$  populations prevail throughout the entire range of RE AS compositions, *i.e.*, not only for those featuring  $n_{\text{Al}} > n_{\text{Si}}$  and/or insufficient modifier contents.<sup>9</sup> The relative amounts of higher-coordination polyhedra were demonstrated to grow for decreasing  $\text{SiO}_2$  content,<sup>9d–f</sup> and particularly when the  $\text{RE}^{3+}$  cation field-strength,  $\text{CFS} = z/R^2$ , is increased,<sup>9b–eg</sup> where  $R$  is the ionic radius. The markedly more cross-linked AS glass network stemming from the higher-coordination  $\text{Al}^{[5]}$  species was recently employed for explaining the progressively enhanced Vickers hardness observed for RE–Al–Si–O glasses with growing CFS according to  $\text{La}^{3+} < \text{Y}^{3+} < \text{Lu}^{3+} < \text{Sc}^{3+}$ .<sup>9e,10</sup> (2) The high positive charge of the  $\text{RE}^{3+}$  cations implies clear violations of the Loewenstein rule, reflected in a pronounced Al/Si atomic disorder for RE AS glass networks, as demonstrated by  $^{29}\text{Si}$  and  $^{27}\text{Al}$  NMR,<sup>9f,11</sup> as well as by molecular dynamics (MD) simulations.<sup>9f,h</sup> Noteworthy, the properties (1) and (2) apply generally to all AS glasses examined thus far from

Physical Chemistry Division, Department of Materials and Environmental Chemistry, Arrhenius Laboratory, Stockholm University, SE-106 91 Stockholm, Sweden.

E-mail: mattias.eden@mmk.su.se

† Electronic supplementary information (ESI) available: Experimental and numerical procedures; examples of best-fit  $^{17}\text{O}$  NMR spectra; additional NMR spectra obtained by strong rf pulses. See DOI: 10.1039/c5cp02985f



the RE = {La, Y, Lu, Sc} systems, regardless of the precise RE/Al/Si composition.<sup>9–11</sup>

Regarding the potential presence of Al<sup>[p]</sup>–NBO contacts, *i.e.*, violation of property (iii) of the prevailing structural picture of (Si-rich) AS glasses, we have recently presented circumstantial experimental evidence by <sup>29</sup>Si NMR of a significant BO/NBO intermixing among SiO<sub>4</sub>/AlO<sub>4</sub> groups in La<sub>2</sub>O<sub>3</sub>–Al<sub>2</sub>O<sub>3</sub>–SiO<sub>2</sub> structures,<sup>11</sup> whereas MD-simulations of Y and Lu bearing glasses reveal that significant fractions (20–50%) of all NBO species are accommodated by AlO<sub>p</sub> groups.<sup>9e</sup> Here we provide the first direct experimental proof of significant Al–NBO contacts in SiO<sub>2</sub>-rich RE<sub>2</sub>O<sub>3</sub>–Al<sub>2</sub>O<sub>3</sub>–SiO<sub>2</sub> glasses with RE = {Y, Lu, Sc}, by utilizing magic-angle spinning (MAS) <sup>17</sup>O NMR. Each specimen was prepared with  $\approx$  20% <sup>17</sup>O-enrichment and is denoted RE<sub>b</sub><sup>a</sup>(r), where *a* and *b* represent the nominal Al<sub>2</sub>O<sub>3</sub> and SiO<sub>2</sub> contents in mol%, respectively, and *r* =  $n_{\text{O}}/(n_{\text{Si}} + n_{\text{Al}})$  conveys the glass network polymerization degree.<sup>1c</sup> All glasses feature 42–65 mol% SiO<sub>2</sub> and  $n(\text{RE}_2\text{O}_3) < n(\text{Al}_2\text{O}_3)$ ; see Table 1. The ESI† describes all sample preparation and basic characterization procedures, as well as the NMR experimentation discussed below.

Fig. 1 displays <sup>17</sup>O MAS NMR spectra recorded from various RE–Al–Si–O glasses with RE = {Y, Lu, Sc} and variable cation compositions, as well as average network polymerization degrees. All NMR spectra manifest two main groups of resonances: one from <sup>17</sup>O<sup>[2]</sup> species—whose peak-maximum ranges between 31–72 ppm and depending primarily on the  $n_{\text{Al}}/n_{\text{Si}}$  molar ratio—and one from NBO ions located at the SiO<sub>4</sub> groups; Si–<sup>17</sup>O<sup>[1]</sup> ( $\sim$  137–158 ppm). While the <sup>17</sup>O<sup>[2]</sup> NMR signal dominates, that from Si–<sup>17</sup>O<sup>[1]</sup> grows concurrently with *r*, *i.e.*, when the glass-network polymerization decreases. Moreover, a weak but significant <sup>17</sup>O resonance appears in the high-ppm region ( $\sim$  175–250 ppm) of all NMR spectra in Fig. 1: it is assigned to Al–<sup>17</sup>O<sup>[1]</sup> motifs. Incidentally, such a signal was previously reported by Schaller and Stebbins in the <sup>17</sup>O MAS NMR spectrum from one Y<sub>2</sub>O<sub>3</sub>–Al<sub>2</sub>O<sub>3</sub>–SiO<sub>2</sub> glass.<sup>9b</sup> However, despite noting that the “NBO peak may include oxygens bonded to AlO<sub>4</sub> or SiO<sub>4</sub> groups” (then referring to the peak herein assigned to Si–<sup>17</sup>O<sup>[1]</sup> groups), they tentatively attributed the high-ppm signal to “NBO species with more yttrium neighbors” than those contributing to the more intense <sup>17</sup>O<sup>[1]</sup> resonance. This <sup>17</sup>O NMR peak appears to be a general feature of high-CFS RE-based AS glasses, but we did not detect it from La<sub>2</sub>O<sub>3</sub>–Al<sub>2</sub>O<sub>3</sub>–SiO<sub>2</sub> glasses (data not shown), in accordance with observations made in ref. 9b.

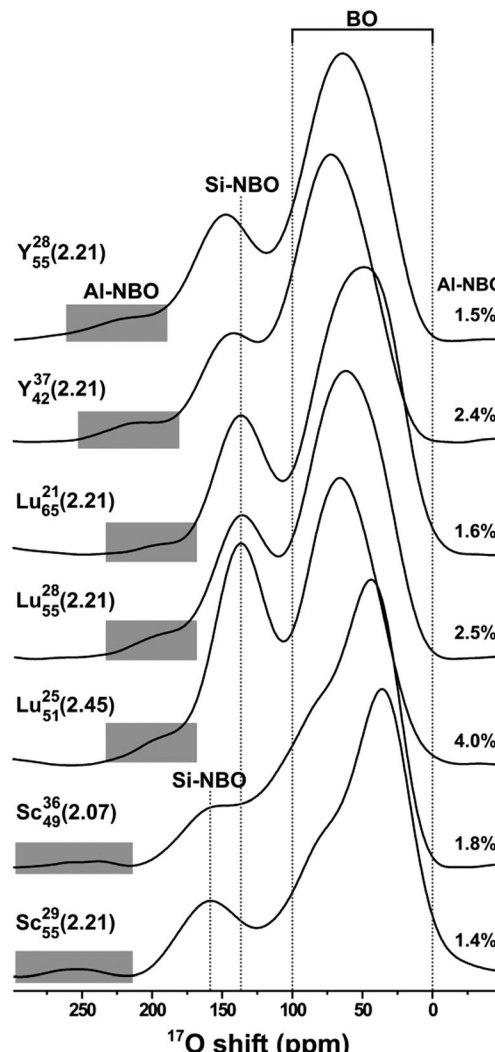


Fig. 1 <sup>17</sup>O MAS NMR spectra recorded from the as-indicated RE<sub>2</sub>O<sub>3</sub>–Al<sub>2</sub>O<sub>3</sub>–SiO<sub>2</sub> glasses at 14.1 T and 24.0 kHz MAS. The signals from BO and Si–NBO moieties are marked by dotted lines, whereas that from Al–NBO is highlighted by a grey rectangle. The relative amounts (in %) of the Al–NBO moieties out of the entire O speciation is indicated at the right portion of each spectrum.

Note that neither the <sup>17</sup>O MAS NMR spectra (Fig. 1) nor their <sup>27</sup>Al counterparts may directly inform about the presence of

Table 1 RE<sub>2</sub>O<sub>3</sub>–Al<sub>2</sub>O<sub>3</sub>–SiO<sub>2</sub> glass compositions and oxygen speciations

Glass compositions <sup>a</sup>				Oxygen populations <sup>b</sup>				NBO populations <sup>c</sup>			
Glass	<i>a</i> RE <sub>2</sub> O <sub>3</sub> (mol%)	<i>b</i> Al <sub>2</sub> O <sub>3</sub> (mol%)	<i>c</i> SiO <sub>2</sub> (mol%)	<i>n</i> <sub>Al</sub> / <i>n</i> <sub>Si</sub>	<i>x</i> <sup>[0]</sup>	<i>x</i> <sup>[1]</sup>	<i>x</i> <sup>[2]</sup>	<i>x</i> <sup>[3]</sup>	<i>x</i> <sup>[1]</sup>	<i>x</i> <sub>Si</sub> <sup>[1]</sup>	<i>x</i> <sub>Al</sub> <sup>[1]</sup>
Y <sub>55</sub> <sup>28</sup> (2.21)	17.05	27.70	55.25	1.00	0.010	0.226	0.653	0.109	0.221 (0.226)	0.206 (0.154)	0.015 (0.072)
Y <sub>42</sub> <sup>37</sup> (2.21)	21.16	37.34	41.50	1.80	0.014	0.232	0.578	0.172	0.210 (0.232)	0.186 (0.119)	0.024 (0.113)
Lu <sub>65</sub> <sup>21</sup> (2.21)	14.50	20.97	64.53	0.65	0.009	0.223	0.684	0.084	0.241 (0.223)	0.224 (0.166)	0.016 (0.056)
Lu <sub>55</sub> <sup>28</sup> (2.21)	17.05	27.70	55.25	1.00	0.013	0.230	0.641	0.115	0.261 (0.230)	0.236 (0.154)	0.025 (0.076)
Lu <sub>51</sub> <sup>25</sup> (2.45)	23.75	25.43	50.82	1.00	0.030	0.329	0.560	0.079	0.369 (0.329)	0.329 (0.212)	0.040 (0.117)
Sc <sub>49</sub> <sup>36</sup> (2.07)	14.77	36.21	49.02	1.48	0.008	0.160	0.610	0.216	0.162 (0.160)	0.144 (0.091)	0.018 (0.069)
Sc <sub>55</sub> <sup>29</sup> (2.21)	16.96	28.48	54.56	1.04	0.017	0.233	0.628	0.121	0.183 (0.233)	0.170 (0.151)	0.014 (0.082)

<sup>a</sup> Nominal *a*RE<sub>2</sub>O<sub>3</sub>–*b*Al<sub>2</sub>O<sub>3</sub>–*c*SiO<sub>2</sub> glass composition with *a* + *b* + *c* = 100 mol%. <sup>b</sup> MD-derived fractional populations of oxygen coordinations {*x*<sup>[*p*]</sup>} with *p* = {0, 1, 2, 3}, where only bonds to Si and Al are counted to define the coordination number *p*. <sup>c</sup> Fractional populations of NBO species (*x*<sup>[1]</sup>) obtained by <sup>17</sup>O MAS NMR, shown together with the contributions from Si–NBO (*x*<sub>Si</sub><sup>[1]</sup>) and Al–NBO (*x*<sub>Al</sub><sup>[1]</sup>) species, where *x*<sup>[1]</sup> = *x*<sub>Si</sub><sup>[1]</sup> + *x*<sub>Al</sub><sup>[1]</sup>. Values within parentheses are the corresponding MD-derived data. The uncertainties are  $\pm 0.015$  and  $\pm 0.010$  for the populations derived from NMR and MD simulations, respectively.



Al-NBO contacts. The  $^{27}\text{Al}$  NMR spectra were recently reported for  $\text{Y}^{9e}$  Lu,  $^{9e}$  and Sc  $^{9g}$  AS glasses, all revealing coexisting  $\text{AlO}_4$ ,  $\text{AlO}_5$ , and  $\text{AlO}_6$  groups. Yet, unambiguous evidence for the assignment of the high-shift  $^{17}\text{O}$  resonance to  $\text{Al}-^{17}\text{O}^{[1]}$  species is provided by the  $^{17}\text{O}\{^{27}\text{Al}\}$  TRAPDOR NMR<sup>12</sup> data presented in Fig. 2. Here the  $^{17}\text{O}-^{27}\text{Al}$  dipolar interaction is recoupled by applying a strong radio-frequency (rf) pulse for  $\tau_{\text{rec}} = 2.5$  ms. For all  $^{17}\text{O}$  sites in close spatial proximity to  $^{27}\text{Al}$ , an attenuated integrated  $^{17}\text{O}$  NMR signal intensity [ $S(\tau_{\text{rec}})$ ] results relative to that observed in the absence of  $^{17}\text{O}-^{27}\text{Al}$  recoupling by using a spin-echo [ $S_0(\tau_{\text{rec}})$ ]. Indeed, due to the presence of Si-O-Al and Al-O-Al structural motifs, the BO-deriving  $^{17}\text{O}$  NMR signals manifest a significant signal dephasing. This also applies to the weak  $^{17}\text{O}$  resonance  $\sim 175$ – $250$  ppm in Fig. 2 (assigned to  $\text{Al}-^{17}\text{O}^{[1]}$  bonds), as is evidenced by its high dephasing ratio  $\Delta S/S_0 = [S_0(\tau_{\text{rec}}) - S(\tau_{\text{rec}})]/S_0(\tau_{\text{rec}})$  obtained by deconvoluting the net  $^{17}\text{O}$  NMR peakshapes, as exemplified for the  $S_0(\tau_{\text{rec}})$  spectra in Fig. 2(b, d and f).

In contrast, the “primary” NBO-stemming resonance reveals no dephasing within the experimental/deconvolution uncertainties; the deconvolution results of Fig. 2(b, d and f) verify that the apparent reduction of this signal stems exclusively from its overlap with the (indeed dephasing)  $^{17}\text{O}^{[2]}$  resonances. This strongly suggests

that the main  $^{17}\text{O}^{[1]}$  NMR peak originates exclusively from Si-NBO fragments, also verifying the absence of contributions from Al-NBO moieties to this signal, as corroborated further by the additional TRAPDOR NMR data shown in Fig. 3. Fig. 3 also includes  $^{17}\text{O}$  NMR spectra recorded by the  $^{27}\text{Al} \rightarrow ^{17}\text{O}$  RAPT-CP technique.<sup>13</sup> In this experiment, solely  $^{17}\text{O}$  species in close proximity to  $^{27}\text{Al}$  are detected. Indeed, while the  $^{17}\text{O}$  resonance-range stemming from BO structural sites is very similar to that observed directly by using central-transition (CT) selective single pulses, no significant NMR-signal intensity is observed in the region  $\gtrsim 125$  ppm that is primarily associated with Si- $^{17}\text{O}^{[1]}$  moieties (note that the weak  $^{27}\text{Al} \rightarrow ^{17}\text{O}$  polarization-transfer efficiency coupled with the low abundance of  $\text{Al}-^{17}\text{O}^{[1]}$  groups precludes their observation).

Each MAS NMR spectrum of Fig. 1 was deconvoluted into signal contributions from  $^{17}\text{O}^{[2]}$ , Si- $^{17}\text{O}^{[1]}$ , and Al- $^{17}\text{O}^{[1]}$  moieties (see the ESI†). The fractional populations are presented in Table 1, together with MD-derived O speciations (see ref. 9e,h).  $^{17}\text{O}$  NMR reveals fractional populations  $x_{\text{Al}}^{[1]} \approx 0.015$ – $0.04$  of Al- $^{17}\text{O}^{[1]}$  species. An overall good agreement is observed between experiments and simulations for the total NBO population ( $x^{[1]} = x_{\text{Si}}^{[1]} + x_{\text{Al}}^{[1]}$ ), the main discrepancy being clearly over-estimated Al-NBO contacts in the glass models. The latter also reveal non-negligible populations of oxygen triclusters ( $x^{[3]}$ ) and “free  $\text{O}^{2-}$  ions” ( $x^{[0]}$ ), as discussed further in ref. 9e,f,h. The attribution of the weak NMR signal to Al- $^{17}\text{O}^{[1]}$  motifs is consistent with the following trends/observations:

(i) As expected from Al-NBO fragments, there is a concomitant increase of  $x_{\text{Al}}^{[1]}$  with the total NBO content in the glass structure (compare the results for  $\text{Lu}^{28}(2.21)$  with  $\text{Lu}^{25}(2.45)$  in Table 1), as well as with the Al content [compare  $\text{Lu}^{21}(2.21)$  and  $\text{Lu}^{28}(2.21)$ ].

(ii) The isotropic chemical shifts associated with the various  $^{17}\text{O}^{[1]}$  sites vary significantly with the nature of the  $\text{RE}^{3+}$  cation, as is also evident from the NMR spectra of Fig. 1. Yet, the Al- $^{17}\text{O}^{[1]}$  isotropic shifts remain consistently  $\sim 60$ – $100$  ppm higher than their Si- $^{17}\text{O}^{[1]}$  counterparts, in qualitative accordance with reported trends of Ca-based aluminate and Si-poor/Ca-rich AS glasses (we stress, however, that no Al-NBO signals were observed for Ca AS glasses exhibiting  $> 20$  mol%  $\text{SiO}_2$ ).<sup>4a,b</sup>

(iii) The low (average) quadrupolar products  $\bar{C}_{Q\eta} = \bar{C}_Q(1 + \eta^2/3)^{1/2} \approx 2.6$  MHz observed for the Si- $^{17}\text{O}^{[1]}$  sites are consistent with previous reports from AS glasses,<sup>1b</sup> whereas the Al- $^{17}\text{O}^{[1]}$  species reveals  $\bar{C}_{Q\eta} \approx 1.7$  MHz (obtained by spectra deconvolution; see the ESI†). This is to our knowledge the first estimate of quadrupolar products for Al- $^{17}\text{O}^{[1]}$  sites. We note that its lower value relative to Si- $^{17}\text{O}^{[1]}$  is expected from the higher ionic character of the Al- $^{17}\text{O}^{[1]}$  bond and consistent with the well-established trend observed for  $^{17}\text{O}^{[2]}$  sites:  $\bar{C}_{Q\eta}(\text{Al-O-Al}) < \bar{C}_{Q\eta}(\text{Al-O-Si}) < \bar{C}_{Q\eta}(\text{Si-O-Si})$ .<sup>1b</sup> The NMR parameters of the various  $^{17}\text{O}$  species will be discussed in detail elsewhere.

To conclude, we have provided the first direct experimental evidence for Al-NBO contacts in highly polymerized  $\text{RE}_2\text{O}_3$ – $\text{Al}_2\text{O}_3$ – $\text{SiO}_2$  glasses with variable RE/Al/Si contents. The results are corroborated by MD simulations. Given the following MD-derived propensity trends of  $\text{AlO}_p$  groups to associate with NBO species,

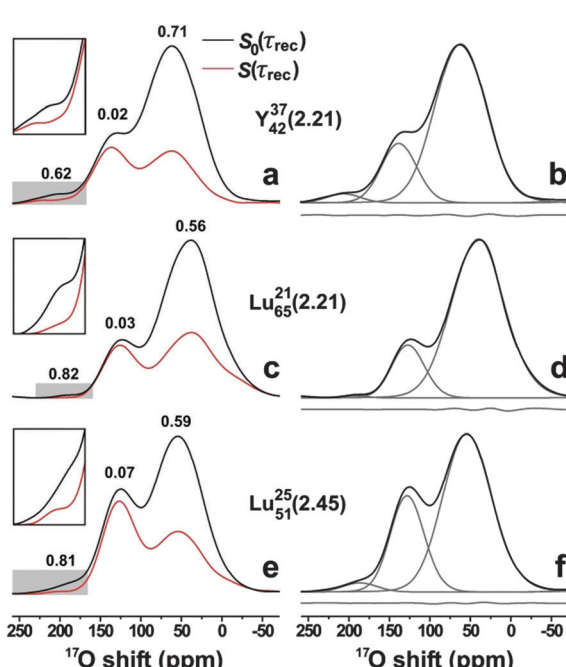
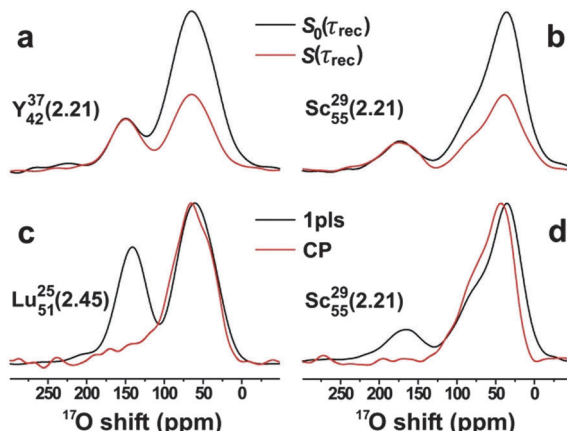


Fig. 2 (a, c, e)  $^{17}\text{O}$  NMR spectra recorded at 9.4 T and 14.0 kHz MAS from the as-indicated Y and Lu bearing AS glasses by employing  $^{17}\text{O}\{^{27}\text{Al}\}$  TRAPDOR NMR.<sup>12</sup> The spectra labelled by  $S(\tau_{\text{rec}})$  and  $S_0(\tau_{\text{rec}})$  were obtained in the presence and absence of dipolar dephasing, respectively ( $\tau_{\text{rec}} = 2.5$  ms). The difference between the black and red traces reflects the degree of  $^{17}\text{O}-^{27}\text{Al}$  contacts among the BO, Al-NBO and Si-NBO species, with the number on top of each signal representing the dephasing degree,  $\Delta S/S_0$  (uncertainty  $\pm 0.03$ ). (b, d, f) Experimental  $S_0(\tau_{\text{rec}})$  NMR spectra (black traces) displayed together with the component peaks (grey traces) obtained by spectra deconvolution. The curves beneath each NMR spectrum in (b, d, f) represents the difference between the experimental and best-fit results.





**Fig. 3**  $^{17}\text{O}$  NMR spectra recorded at 14.1 T from the as-indicated RE AS glasses by employing (a, b)  $^{17}\text{O}\{^{27}\text{Al}\}$  TRAPDOR<sup>12</sup> and (c, d)  $^{27}\text{Al} \rightarrow ^{17}\text{O}$  RAPT-CP<sup>13</sup> NMR experiments, the latter shown together with results obtained by CT-selective pulses ("1pls"). The data were collected at MAS rates of (a, b) 24.0 kHz and (c, d) 14.0 kHz, by using 3.2 mm and 4.0 mm triple-resonance MAS probeheads, respectively. The two NMR spectra in each of (a, b) are shown on the same absolute intensity scale, whereas those in (c, d) are scaled to display equal peak maxima of the  $^{17}\text{O}^{[2]}$  resonances.

$\text{AlO}_4 > \text{AlO}_5 > \text{AlO}_6$ ,<sup>9h</sup> we attribute most of the Al-associated NBO species to be located at  $\text{AlO}_4$  tetrahedra. Notwithstanding a strong preference for  $\text{SiO}_4$  groups to accommodate the NBO ions, the presence of Al-NBO moieties of  $\lesssim 4\%$  out of the total O speciation (7–11% of all NBO) appears to be a general feature of AS glasses that incorporate trivalent cations with high field strength: apparently they stabilize otherwise energetically disfavoured structural motifs.

While the relative Al-NBO populations grow concurrently with the Al content of the glass, they persist in  $\text{SiO}_2$ -rich networks (at least up to  $\approx 65$  mol%  $\text{SiO}_2$ ), despite that their net NBO population remain relatively low ( $x^{[1]} \approx 0.22$ ). This is in stark contrast to AS glasses based on low-CFS mono/divalent cations, where non-negligible Al-NBO contacts have hitherto only been observed directly for fragmented networks rich in modifiers ( $\gtrsim 50$  mol%  $\text{M}_{(2)}\text{O}$ ) and simultaneously featuring low  $\text{SiO}_2$  ( $\lesssim 30$  mol%) contents and high molar ratios  $n(\text{Al}_2\text{O}_3)/n(\text{SiO}_2) > 2$ .<sup>4a</sup>

This work was supported by the Carl Trygger Foundation, the Magn. Bergvall Foundation, and the Swedish Research Council (contract VR-NT 2010-4943). We gratefully acknowledge NMR equipment grants from the Swedish Research Council and the Knut and Alice Wallenberg Foundation.

## Notes and references

- (a) G. Engelhardt and D. Michel, *High-resolution solid-state NMR of silicates and zeolites*, John Wiley, Chichester, UK, 1987; (b) K. J. D. MacKenzie and M. E. Smith, *Multinuclear solid-state NMR of inorganic materials*, Pergamon Press, Amsterdam, 2002; (c) M. Edén, *Annu. Rep. Prog. Chem., Sect. C: Phys. Chem.*, 2012, **108**, 177.
- (a) B. O. Mysen, D. Virgo and I. Kushiro, *Am. Mineral.*, 1981, **66**, 678; (b) J. B. Murdoch, J. F. Stebbins and I. S. E. Carmichael, *Am. Mineral.*, 1985, **70**, 332; (c) C. I. Merzbacher, B. L. Sherriff, J. S. Hartman and W. B. White, *J. Non-Cryst. Solids*, 1990, **124**, 194.
- W. Lowenstein, *Am. Mineral.*, 1954, **39**, 92.
- (a) J. R. Allwardt, S. K. Lee and J. F. Stebbins, *Am. Mineral.*, 2003, **88**, 949; (b) S. K. Lee and J. F. Stebbins, *Geochim. Cosmochim. Acta*, 2006, **70**, 4275; (c) D. R. Neuville, L. Cormier and D. Massiot, *Chem. Geol.*, 2006, **229**, 173.
- (a) J. F. Stebbins, S. Kroeker, S. K. Lee and T. J. Kiczenski, *J. Non-Cryst. Solids*, 2000, **275**, 1; (b) M. J. Toplis, S. C. Kohn, M. E. Smith and I. J. F. Poplett, *Am. Mineral.*, 2000, **85**, 1556.
- S. K. Lee, *Solid State Nucl. Magn. Reson.*, 2010, **38**, 45.
- (a) S. K. Lee and J. F. Stebbins, *J. Phys. Chem. B*, 2000, **104**, 4091; (b) S. K. Lee and J. F. Stebbins, *J. Non-Cryst. Solids*, 2000, **270**, 260.
- (a) A. Makishima, M. Kobayashi, T. Shimohira and T. Nagata, *J. Am. Ceram. Soc.*, 1982, **65**, C210; (b) J. T. Kohli and J. E. Shelby, *Phys. Chem. Glasses*, 1991, **32**, 67.
- (a) J. T. Kohli, J. E. Shelby and J. S. Frye, *Phys. Chem. Glasses*, 1992, **33**, 73; (b) T. Schaller and J. F. Stebbins, *J. Phys. Chem. B*, 1998, **102**, 10690; (c) S. Iftekhar, J. Grins, P. N. Gunawidjaja and M. Edén, *J. Am. Ceram. Soc.*, 2011, **94**, 2429; (d) P. Florian, N. Sadiki, D. Massiot and J. P. Coutures, *J. Phys. Chem. B*, 2007, **111**, 9747; (e) S. Iftekhar, B. Pahari, K. Okhotnikov, A. Jaworski, B. Stevensson, J. Grins and M. Edén, *J. Phys. Chem. C*, 2012, **116**, 18394; (f) A. Jaworski, B. Stevensson, B. Pahari, K. Okhotnikov and M. Edén, *Phys. Chem. Chem. Phys.*, 2012, **14**, 15866; (g) B. Pahari, S. Iftekhar, A. Jaworski, K. Okhotnikov, K. Jansson, B. Stevensson, J. Grins and M. Edén, *J. Am. Ceram. Soc.*, 2012, **95**, 2545; (h) K. Okhotnikov, B. Stevensson and M. Edén, *Phys. Chem. Chem. Phys.*, 2013, **15**, 15041.
- B. Stevensson and M. Edén, *J. Non-Cryst. Solids*, 2013, **378**, 163.
- S. Iftekhar, E. Leonova and M. Edén, *J. Non-Cryst. Solids*, 2009, **355**, 2165.
- C. P. Grey and W. S. Veeman, *Chem. Phys. Lett.*, 1992, **192**, 379.
- M. Edén, J. Grins, Z. Shen and Z. Weng, *J. Magn. Reson.*, 2004, **169**, 279.

